Groovy Drops: Effect of Groove Curvature on Spontaneous Capillary Flow

Myra Kitron-Belinkov,[†,||] Abraham Marmur,*[,†] Thomas Trabold,[‡] and Gayatri Vyas Dadheech[§]

Department of Chemical Engineering, Technion - Israel Institute of Technology, 32000 Haifa, Israel, General Motors Fuel Cell Activities, Honeoye Falls, New York 14472, and General Motors Fuel Cell Activities, Warren, Michigan 48090

Received February 17, 2007. In Final Form: May 23, 2007

Spontaneous capillary flow (SCF) of a drop in a groove with an ideally sharp corner is possible when the Concus-Fin (CF) condition is fulfilled. However, since ideally sharp corners do not exist in reality, it is important to understand the effect of finite corner curvature on SCF. This effect is analytically studied for long drops in a V-shaped groove with a curved corner, leading to a generalization of the CF condition for such drops. The generalized condition implies that SCF depends on the geometry of the corner as well as on the dimensionless length of the drop, in addition to its dependence on the opening angle and contact angle that is covered by the CF condition. Specific calculations are presented for rounded corners. In addition, this effect is numerically calculated for short drops in V-shaped grooves with rounded corners, using the *Surface Evolver* software. The results of both types of calculations show that even a relatively small corner radius strongly affects the possibility of SCF: when the corner is not ideally sharp, SCF requires conditions that are more difficult to achieve than predicted by the CF condition; also, the spreading of the drop stops at a finite length and does not proceed indefinitely.

Introduction

Flow along grooves and in angular capillaries is frequently encountered in applications related to a variety of fields, such as nanotechnology, fuel cells, and space technology.[1−6] The spontaneity of such flows, when the corner of the groove or capillary is ideally sharp, is determined by the Concus-Finn (CF) condition,[7−18] which states that spontaneous capillary flow (SCF) occurs when $\beta > \theta$, where θ is the ideal (Young) contact angle that the liquid makes with the solid wall, and

$$\beta \equiv (\pi - \alpha)/2 \tag{1}$$

where α is the opening angle of the groove or capillary corner. When $\beta < \theta$, the liquid interface may have a unique stable configuration.

The CF condition is universal for various system geometries, providing they have ideally sharp corners. However, real grooves or capillaries cannot be made perfectly sharp. It has been known for a long time that roundness of the corner mitigates the spontaneity of the capillary flow,[8,9,13,17,18] but this effect seems to be geometry-dependent. The present paper focuses on liquid drops in grooves; therefore, its objective is to generalize the CF condition for a drop in a groove of a general shape. To achieve this objective, two approaches are taken. In the first approach, the condition for SCF is analytically formulated for long drops in a groove of a general shape and demonstrated for rounded groove corners. Next, three-dimensional calculations of drops in sharp and rounded grooves are presented, based on calculations done with the *Surface Evolver*.[19,20] The results show a strong dependence of the SCF condition on the roundness of the groove corner and an appreciable dependence on the (dimensionless) length of the drop.

Long Drops

In this section, the condition for SCF of a long drop in a groove is analytically developed. This will serve as a basis for comparison with the case of a short drop, which must be numerically calculated in three dimensions, and will be presented in the next section. The assumption of long drops not only makes the analysis much easier, but is justified for a very simple reason: when a drop spontaneously flows in a groove, it becomes elongated; thus, the completion of the SCF always involves long drops. The groove to be discussed here is basically V-shaped, with a corner that may be curved in a general way, as shown in Figure 1a along with the geometrical definitions. This general group of groove shapes covers many of the cases encountered in practice.

The V-shape of the groove is characterized by its complementary opening angle, β (see Figure 1a and eq 1). The difference

* Fax: 972-4-829-3088. E-mail: marmur@technion.ac.il.
† Technion - Israel Institute of Technology.
‡ General Motors Fuel Cell Activities, Honeoye Falls, New York.
§ General Motors Fuel Cell Activities, Warren, Michigan.
|| Present address: School of Engineering, Kinneret College on the Sea of Galilee, Emek-Hayarden, 15132 Israel.

(1) Stone, H. A.; Stroock, A. D.; Ajdari, A. *Annu. Rev. Fluid Mech.* **2004**, *36*, 381−411.
(2) Zhao, B.; Moore, J. S.; Beebe, D. J. *Science* **2001**, *291*, 1023−1026.
(3) Concus, P.; Finn, R.; Weislogel, M. *Exp. Fluids* **2000**, *28*, 197−205.
(4) Trabold, T. A. *Heat Transfer Eng.* **2005**, *26*, 3−12.
(5) Yang, X. G.; Zhang, F. Y.; Lubawy, A. L.; Wang, C. Y. *Electrochem. Solid State Lett.* **2004**, *7* (11), A408−A411.
(6) Seeman, R.; Brinkmann, M.; Kramer, E. J.; Lange, F. F.; Lipowski, R. *Proc. Natl. Acad. Sci. U.S.A.* **2005**, *102* (6), 1848−1852.
(7) Concus, P.; Finn, R. *Appl. Math. Sci.* **1969**, *63*, 292−299.
(8) Concus, P.; Finn, R. *Microgravity Sci. Technol.* **1990**, *3* (2), 87−92.
(9) De Ramos, A. L.; Cerro, R. L. *Chem. Eng. Sci.* **1994**, *49* (14), 2395−2398.
(10) Dong, M.; Chatzis, I. *J. Colloid Interface Sci.* **1995**, *172*, 278−288.
(11) Romero, L. A.; Yost, F. G. *J. Fluid Mech.* **1996**, *322*, 109−129.
(12) Rye, R. R.; Mann, J. A., Jr.; Yost, F. G. *Langmuir* **1996**, *12*, 555−565.
(13) Rye, R. R.; Yost, F. G.; O'Toole, E. J. *Langmuir* **1998**, *14*, 3937−3943.
(14) Popov, Y. O.; Witten, T. A. *Eur. Phys. J. E* **2001**, *6*, 211−220.
(15) Bico, J.; Quere, D. *J. Colloid Interface Sci.* **2002**, *247* (1), 162−166.
(16) Brinkmann, M.; Blossey, R. *Eur. Phys. J. E* **2004**, *14*, 79−89.
(17) Parry, A. O.; Rascon, C. *J. Chem. Phys.* **2005**, *123*, paper no. 234105.
(18) Brady, V.; Concus, P.; Finn, R. *Microgravity Sci. Technol.* **2004**, *15*, 31−38.
(19) Brakke, K. A. *Exp. Math.* **1992**, *1* (2), 141−165.
(20) Collicott, S. H.; Weislogel, M. M. *AIAA J.* **2004**, *42* (2), 289−295.

10.1021/la700473m CCC: $37.00
Published on Web 07/04/2007 PAGE EST: 4.1

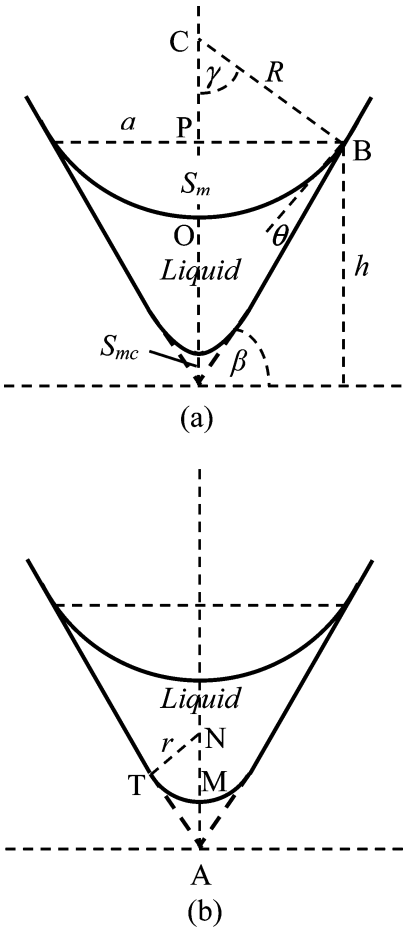

Figure 1. (a) A basically V-shaped groove, with a generally curved corner. (b) A rounded corner smoothly connected to the straight walls of the groove.

between the cross-sectional area of the V-shaped groove and that of the curved-corner groove is S_{mc} (S_{mc} is defined to be positive when the latter is smaller than the former). The difference between the length of the solid−liquid perimeter in the curved-corner groove and that in the V-shaped groove is p (p is defined to be positive when the latter is smaller than the former). The drop is assumed to be sufficiently long, so that the shape of its edges does not greatly affect the energy of the system; therefore, the effect of the drop edges is neglected. The drop is characterized by its length, l, its fixed volume, V, and the contact angle, θ. In most applications of drops in grooves, the drop is sufficiently small for gravity to be neglected, since the typical size of the drop is much smaller than the capillary constant, $\sqrt{2\sigma/(\rho g)}$, which is on the order of magnitude of a few millimeters, where σ is the surface tension of the liquid, ρ is the density of the liquid, and g is the gravitational acceleration. In addition, the present analysis ignores the effect of contact angle hysteresis, since it does not affect the main message of this communication.

The interfacial energy of the system, G, is given by

$$G = \sigma S_{lv} + (\sigma_{sl} - \sigma_s)S_{sl} \tag{2}$$

where σ_{sl} is the solid−liquid interfacial tension, σ_s is the surface tension of the solid, and S_{lv} and S_{sl} are the liquid−air and solid−liquid interfacial areas, respectively. In order to decrease the number of parameters in the equation, the dimensionless interfacial energy, G^*, defined by the following equation, will be used

$$G^* = \frac{G}{\sigma V^{2/3}} = S^*_{lv} - S^*_{ls}\cos\theta \tag{3}$$

where $S^*_{lv} \equiv S_{lv}/V^{2/3}$, $S^*_{sl} \equiv S_{sl}/V^{2/3}$, and $\cos\theta = (\sigma_s - \sigma_{sl})/\sigma$, by the Young equation. If the liquid−air and solid−liquid areas are expressed in terms of the parameters that define the groove and the liquid (see the Appendix for the details), the expression for G^* becomes

$$G^* = 2(l^{*-1} + S^*_{mc})^{1/2} l^* \left(\tan\beta + \frac{1}{\tan\gamma} - \frac{\gamma}{\sin^2\gamma}\right)^{-1/2} \times \left(\frac{\gamma}{\sin\gamma} - \frac{\cos\theta}{\cos\beta}\right) - l^* p^* \cos\theta \tag{4}$$

where $l^* \equiv l/V^{1/3}$ is the dimensionless drop length, $p^* \equiv p/V^{1/3}$, and $\gamma = \beta - \theta$. The condition for SCF of the drop can be formulated in a straightforward way: in order for the flow to be spontaneous, G^* has to decrease when the length of the drop increases. In other words, the derivative of the energy with respect to the length of the drop must then be negative

$$\frac{\partial G^*}{\partial l^*} = 2(l^{*-1} + S^*_{mc})^{1/2}\left[1 - \frac{1}{2} l^{*-1}(l^{*-1} + S^*_{mc})^{-1}\right]\left(\tan\beta + \frac{1}{\tan\gamma} - \frac{\gamma}{\sin^2\gamma}\right)^{-1/2}\left(\frac{\gamma}{\sin\gamma} - \frac{\cos\theta}{\cos\beta}\right) - p^*\cos\theta < 0 \tag{5}$$

For a V-shaped groove, $S_{mc} = 0$, $p = 0$, and the condition for SCF is

$$\frac{\partial G^*}{\partial l^*} = l^{*-1/2}\left(\tan\beta + \frac{1}{\tan\gamma} - \frac{\gamma}{\sin^2\gamma}\right)^{-1/2} \times \left(\frac{\gamma}{\sin\gamma} - \frac{\cos\theta}{\cos\beta}\right) < 0 \tag{6}$$

The factor $l^{*-1/2}$ is always positive. When $\theta \to \beta$, i.e., $\gamma \to 0$, the sum of the second and third terms within the first pair of brackets goes to zero, and $\tan\beta$ is positive (since our main interest is positive β). The expression in the second pair of brackets approaches zero when $\theta \to \beta$ ($\gamma \to 0$) and is negative for $\theta < \beta$. Therefore, the energy decreases as l increases if and only if $\beta > \theta$. Thus, the drop spontaneously flows along the groove if the contact angle is smaller than the complementary opening angle. This condition is actually the CF condition,[7] which is independent of the drop length.

However, the situation is quite different for flow in a groove with a curved corner. Equation 5 serves as the generalized CF condition for a long drop in such a groove. This equation shows that the condition for SCF for a groove with a curved corner may, in general, depend on the geometry of the corner and on the length of the drop. As a demonstration that will be followed later by numerical calculations for short drops, it is of interest to see the effect of rounded corners. A rounded corner may serve as a very reasonable simplified model for real grooves that are meant to be V-shaped as much as possible but cannot be made so because of the limitations of cutting tools. Figure 1b shows a rounded corner, which is defined by a circle of radius r that is smoothly connected to the walls of the groove (the walls are tangent to the circle at the connection point). The "missing" cross section of the corner is (see Figure 1b)

$$S^*_{mc} = 2(S_{ATN} - S_{MTN})/V^{2/3} = r^{*2}(\tan\beta - \beta) \tag{7}$$

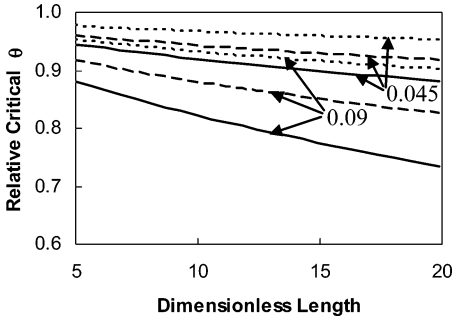

Figure 2. Relative critical contact angle vs dimensionless length of drop. The numbers near the arrows show the dimensionless corner radii. The complementary groove angles, β, are as follows: 60° (—), 45° (---), and 30° (···).

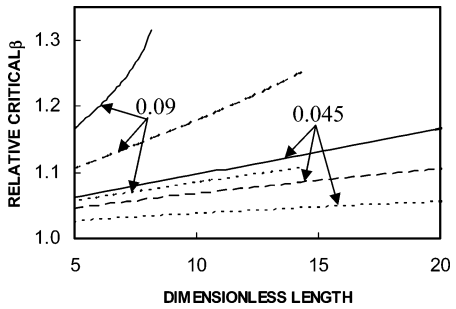

Figure 3. Relative critical complementary groove angle vs dimensionless length of drop. The numbers near the arrows show the dimensionless corner radii. The contact angles, θ, are as follows: 60° (—), 45° (---), and 30° (···).

where $r^* \equiv r/V^{1/3}$ is the dimensionless corner radius. The difference between the solid−liquid cross section perimeters of the rounded and V-shaped grooves is given by

$$p^* = 2r^*(\beta - \tan\beta) \tag{8}$$

Substituting eqs 7 and 8 into eq 5 allows the calculation of the condition for SCF for a rounded corner.

Sample results of such calculations are shown in Figures 2 and 3. The former applies to the case where the groove opening angle is set (β is given), and one seeks to determine the critical (highest) contact angle that assures SCF according to eq 5. Figure 3 shows results for the case where θ is set and one looks for the critical (lowest) β. In both figures the critical angles are shown relative to the corresponding CF critical values (i.e., $\theta = \beta$): the relative critical θ is defined as the critical θ divided by β; the relative critical β is defined as the critical β divided by θ. Two values of r^* (0.045 and 0.09) and three values of either β or θ (30°, 45°, and 60°) are used in the calculations. These results demonstrate, in general, that it is more difficult (requires a lower θ or higher β) to ensure SCF in a rounded groove than it is for a sharp, V-shaped one. The effect of rounding the corner turns out to be significant, especially for determining the critical β for a given θ. Also, Figures 2 and 3 show that the critical angle for SCF depends on the length of the drop: as the drop flows and becomes longer and longer, the requirement for SCF becomes more difficult to achieve. This result further justifies the use of the simplifying assumption of long drops, since it shows that a SCF criterion that holds for long drops will necessarily hold for short drops. Thus, it turns out that the general condition for SCF depends not only on the parameters that determine the system, but also on the temporary state of the system (length of the drop). In other words, even if the drop starts to spontaneously flow along the groove, it will reach a length at which the spontaneous flow will be arrested. This is in marked contrast to the theoretically expected results for an ideal V-shaped groove.

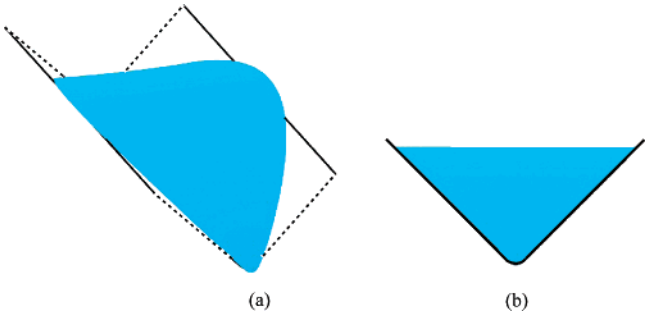

Figure 4. The equilibrium shape of a drop in a groove with $\beta = 45°$ and $r^* = 0.16$. $\theta = 45°$: (a) a three-dimensional view; the dimensionless length of the frame is 9.6. (b) a cross-sectional view. The dashed lines represent "cuts" through the groove walls, to indicate that these walls continue indefinitely.

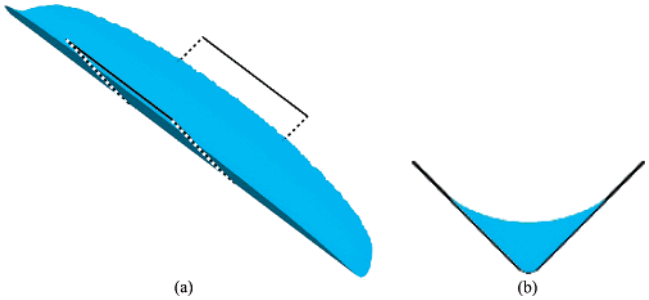

Figure 5. As in Figure 4; however, $\theta = 10°$. The drop did not reach an equilibrium configuration when the calculation was stopped.

Short Drops

In this section, the previous theoretical analysis for long drops is complemented by numerical, three-dimensional calculations for short drops within grooves with sharp and rounded corners. The calculations were done using the *Surface Evolver* software.[19,20] To perform the calculations, the contact angle on the wall faces of the evolving body was prescribed, through the definition of relevant surface tensions (the surface integral method). The main quantitative condition for the convergence of the results was the comparison between the prescribed contact angle and the calculated mean contact angle along the evolving surface. The calculations were performed for corners with values of r^*, the dimensionless corner radius, between 0 (an ideal V-shaped corner) and 0.49. Grooves with three complementary opening angles, $\beta = 30°$, 45°, and 60°, were compared. For each groove, contact angles below and above β, the CF critical value, were used.

Since the *Surface Evolver* software can be used only for equilibrium calculations, the dynamic process of imbibition cannot be followed by it. However, the existence of imbibition can be suspected if the system does not converge to an equilibrium state. Therefore, the first answer needed from the calculations was, does the system reach equilibrium? If it does, then the details of the equilibrium state were elucidated. Practically, equilibrium was considered to have been reached if all calculated contact angles were different from the prescribed one by less than 3° and the length of the drop approached a constant value. In some cases, it was very easy to decide that a given configuration was an equilibrium state, since within a limited number of iterations, these criteria were met. An example is shown in Figure

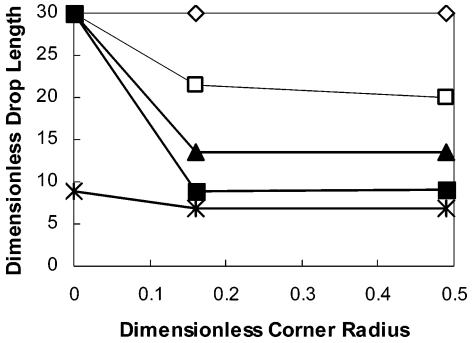

Figure 6. The dimensionless drop length vs the dimensionless corner radius for $\beta = 60°$. The values of θ are as follows: ♢, 10°; □, 30°; ▲, 45°; ■, 60°; *, 75°. A dimensionless length of 30 indicates that the calculations were stopped because they were not converging to an equilibrium state.

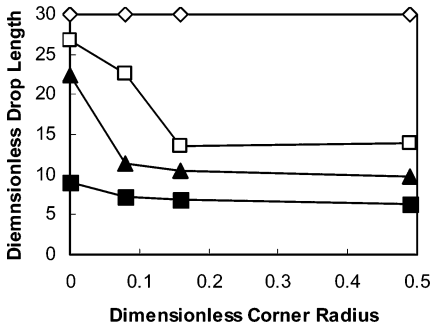

Figure 7. The dimensionless drop length vs the dimensionless corner radius for $\beta = 45°$. The values of θ are as follows: ♢, 10°; □, 30°; ▲, 45°; ■, 60°. A dimensionless length of 30 indicates that the calculations were stopped because they were not converging to an equilibrium state.

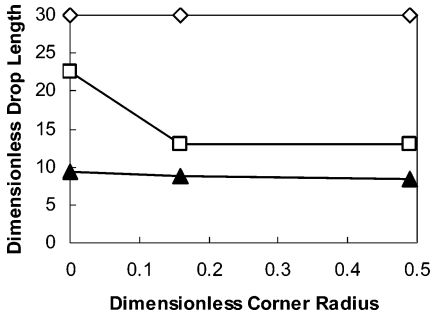

Figure 8. The dimensionless drop length vs the dimensionless corner radius for $\beta = 30°$. The values of θ are as follows: ♢, 10°; □, 30°; ▲, 45°. A dimensionless length of 30 indicates that the calculations were stopped because they were not converging to an equilibrium state.

4. In other cases, the answer was more difficult to get, since even after thousands of iterations with refined surface triangulations, the calculated contact angle was still different from the prescribed one, and the drop continued to elongate. An example for this situation is shown in Figure 5. Most of the calculations were redone a number of times, varying the initial configuration of the drop or the initial steps of the calculation, in order to verify repeatability.

The results of the performed calculations are summarized in Figures 6−8, which show the final dimensionless drop length vs the dimensionless corner radius. In cases where the dimensionless length exceeded 30, the calculations were stopped, and the results were artificially put to be 30 (assuming the drop continued to imbibe into the groove). These figures clearly indicate that indeed the CF condition is fulfilled for ideal V-shaped grooves, a fact that adds credibility to the numerical calculations. In addition, these figures show that roundness of the corner has a major effect on SCF in the groove: the drop may get to equilibrium even for contact angles that are much lower than β, the CF critical value. These numerical observations support the conclusions reached analytically for long drops.

Summary and Conclusions

The condition for spontaneous capillary flow (SCF) of a drop in a groove with a curved corner was analytically developed for long drops (eq 5), as well as numerically studied for short drops. The present analytical condition serves as a generalization of the CF condition (that is universal for ideally sharp corners) to the case of a drop in a real groove, which cannot be made ideally sharp. The generalized condition shows that SCF strongly depends on the geometry of the corner and on the length of the drop, in addition to its dependence on the opening angle and contact angle that is covered by the CF condition. The results of both analyses show that even relatively small corner radii (such as less than 10% of the groove opening) strongly affect the possibility of SCF in this system. In general, the results indicate that, when the corner is not ideally sharp, the spreading of the drop stops at a finite length and does not proceed indefinitely; in addition, the condition for SCF in this case is more difficult to achieve than the CF condition.

Acknowledgment. This research was partially funded by the General Motors Corporation under GM-UMIT R&D project collaboration.

Appendix

Derivation of the General Expression for a Curved Groove. The cross section of the drop, *S*, is given by

$$S = V/l \tag{A1}$$

Geometrically, this area is given by (see definitions in Figure 1a)

$$S = ah - S_{\mathrm{m}} - S_{\mathrm{mc}} \tag{A2}$$

where a is the distance BP, h is the height of B above the edge of the V-shaped groove, and S_{m} is given by

$$S_{\mathrm{m}} = 2(S_{\mathrm{COB}} - S_{\mathrm{CPB}}) = \gamma R^2 - Ra\cos\gamma \tag{A3}$$

where (see Figure 1a) R is the radius of the liquid−air meniscus, and

$$\gamma = \beta - \theta \tag{A4}$$

Also,

$$R = \frac{a}{\sin(\beta - \theta)} \tag{A5}$$

so that when eqs A3−A5 are substituted in eq A2 one gets

$$S_{\mathrm{m}} = a^2 \frac{1}{\sin\gamma}\left(\frac{\gamma}{\sin\gamma} - \cos\gamma\right) \tag{A6}$$

Since

$$h = a\tan\beta \tag{A7}$$

then substitution of A7 and A6 into A2 and A1 yields

$$a = \left(\frac{V}{l} + S_{\mathrm{mc}}\right)^{1/2}\left(\tan\beta + \frac{1}{\tan\gamma} - \frac{\gamma}{\sin^2\gamma}\right)^{-1/2} \tag{A8}$$

Using eqs A4, A5, and A8, the liquid−air area can be expressed as

$$S_{lv} = 2\gamma Rl = 2\frac{\gamma l}{\sin\gamma}\left(\frac{V}{l} + S_{mc}\right)^{1/2}\left(\tan\beta + \frac{1}{\tan\gamma} - \frac{\gamma}{\sin^2\gamma}\right)^{-1/2} \quad \text{(A9)}$$

The solid−liquid area may be expressed as

$$S_{sl} = \left(2\frac{a}{\cos\beta} + p\right)l = 2\frac{l}{\cos\beta}\left(\frac{V}{l} + S_{mc}\right)^{1/2}\left(\tan\beta + \frac{1}{\tan\gamma} - \frac{\gamma}{\sin^2\gamma}\right)^{-1/2} + pl \quad \text{(A10)}$$

Finally, substitution of A9 and A10 into eq 3 leads to eq 4. The equation is valid for $\gamma \geq 0$ and for $\gamma < 0$, but the latter is of no practical interest.

LA700473M